

EUR Research Information Portal

Structural disconnectivity and the risk of dementia in the general population

Published in:
Neurology

Publication status and date:
Published: 01/01/2020

DOI (link to publisher):
[10.1212/WNL.00000000000010231](https://doi.org/10.1212/WNL.00000000000010231)

Document Version
Publisher's PDF, also known as Version of record

Citation for the published version (APA):

Cremers, L., Wolters, F., de Groot, M., Ikram, K., van der Lugt, A., Niessen, W., Vernooij, M., & Ikram, A. (2020). Structural disconnectivity and the risk of dementia in the general population. *Neurology*, *95*(11), e1528-e1537. <https://doi.org/10.1212/WNL.00000000000010231>

[Link to publication on the EUR Research Information Portal](#)

Terms and Conditions of Use

Except as permitted by the applicable copyright law, you may not reproduce or make this material available to any third party without the prior written permission from the copyright holder(s). Copyright law allows the following uses of this material without prior permission:

- you may download, save and print a copy of this material for your personal use only;
- you may share the EUR portal link to this material.

In case the material is published with an open access license (e.g. a Creative Commons (CC) license), other uses may be allowed. Please check the terms and conditions of the specific license.

Take-down policy

If you believe that this material infringes your copyright and/or any other intellectual property rights, you may request its removal by contacting us at the following email address: openaccess.library@eur.nl. Please provide us with all the relevant information, including the reasons why you believe any of your rights have been infringed. In case of a legitimate complaint, we will make the material inaccessible and/or remove it from the website.

Structural disconnectivity and the risk of dementia in the general population

Lotte G.M. Creemers, PhD, Frank J. Wolters, MD, Marius de Groot, PhD, M. Kamran Ikram, PhD, Aad van der Lugt, PhD, Wiro J. Niessen, PhD, Meike W. Vernooij, PhD,* and M. Arfan Ikram, PhD*

Neurology® 2020;95:e1528-e1537. doi:10.1212/WNL.0000000000010231

Correspondence

Dr. Ikram
m.a.ikram@erasmusmc.nl

Abstract

Objective

The disconnectivity hypothesis postulates that partial loss of connecting white matter fibers between brain regions contributes to the development of dementia. Using diffusion MRI to quantify global and tract-specific white matter microstructural integrity, we tested this hypothesis in a longitudinal population-based study.

Methods

Global and tract-specific fractional anisotropy (FA) and mean diffusivity (MD) were obtained in 4,415 people without dementia (mean age 63.9 years, 55.0% women) from the prospective population-based Rotterdam Study with brain MRI between 2005 and 2011. We modeled the association of these diffusion measures with risk of dementia (follow-up until 2016) and with changes on repeated cognitive assessment after on average 5.4 years, adjusting for age, sex, education, macrostructural MRI markers, depressive symptoms, cardiovascular risk factors, and *APOE* genotype.

Results

During a median follow-up of 6.8 years, 101 participants had incident dementia, of whom 83 had clinical Alzheimer disease (AD). Lower global values of FA and higher values of MD were associated with an increased risk of dementia (adjusted hazard ratio [95% confidence interval (CI)] per SD increase for MD 1.79 [1.44–2.23] and FA 0.65 [0.52–0.80]). Similarly, lower global values of FA and higher values of MD related to more cognitive decline in people without dementia (difference in global cognition per SD increase in MD [95% CI] was –0.04 [–0.07 to –0.01]). Associations were most profound in the projection, association, and limbic system tracts.

Conclusions

Structural disconnectivity is associated with an increased risk of dementia and more pronounced cognitive decline in the general population.

*These authors contributed equally to this work.

From the Departments of Radiology and Nuclear Medicine (L.G.M.C., F.J.W., M.d.G., A.v.d.L., W.J.N., M.W.V.), Epidemiology (L.G.M.C., F.J.W., M.d.G., M.K.I., M.W.V., M.A.I.), Neurology (F.J.W., M.K.I., M.A.I.), and Medical Informatics (M.d.G., W.J.N.), Erasmus MC, Rotterdam; and Department of Imaging Physics, Faculty of Applied Sciences (W.J.N.), Delft University of Technology, Delft, the Netherlands.

Go to [Neurology.org/N](https://www.neurology.org/N) for full disclosures. Funding information and disclosures deemed relevant by the authors, if any, are provided at the end of the article.

Glossary

AD = Alzheimer disease; **BMI** = body mass index; **CES-D score** = Center for Epidemiologic Studies Depression Scale; **DSM-III-R** = *Diagnostic and Statistical Manual of Mental Disorders, 3rd edition, revised*; **FA** = fractional anisotropy; **FLAIR** = fluid-attenuated inversion recovery; **GMS** = Geriatric Mental Schedule; **HDL** = high-density lipoprotein; **HR** = hazard ratio; **ICV** = intracranial volume; **MD** = mean diffusivity; **MMSE** = Mini-Mental State Examination; **WMH** = white matter hyperintensity.

Dementia is among the leading causes of death and disability worldwide, and its socioeconomic burden on society will continue to increase as the number of persons with dementia is predicted to nearly triple to 131 million in 2050.¹ Effective preventive and curative interventions are urgently needed, but their development and timely application is hampered by incomplete understanding of pathophysiology, lack of markers that can identify changes in the very early, subclinical stages of disease, and lack of prognostic markers. Subclinical brain changes are thought to occur years, if not decades, prior to onset of clinical symptoms,² which is beyond the scope of currently applied subclinical macrostructural imaging markers of neurodegeneration, such as hippocampal volume and presence of white matter hyperintensities (WMHs). Despite advances in measurement of amyloid and tau, these measurements come at high cost and provide incomplete answers to prediction of dementia in the presence of a multitude of pathologies at old age.³ In particular, when selecting individuals in the community for further screening or trial inclusion, imaging tools are valuable to improve prognostic precision beyond clinical characteristics.⁴

One of the recent insights in dementia is that brain damage can lead to disruption of brain networks, so called disconnectivity.^{5–7} Disconnectivity, which can be investigated using diffusion MRI, seems to occur prior to changes in conventional structural MRI markers such as WMHs load in dementia,⁸ and is thought to reflect early cerebral white matter damage.^{9,10} Disconnectivity is more pronounced in patients with dementia compared to healthy controls,^{11,12} and relates to more rapid cognitive decline in patients with Alzheimer disease (AD).¹³ In 4 longitudinal studies from 2 clinical cohorts of patients with small vessel disease, network disruption was related to accelerated decline in psychomotor speed and an increased risk of dementia.^{14–17} However, patients with substantial small vessel disease on MRI represent a minority of the individuals at high risk of dementia in the community, and it remains undetermined whether prior findings extend to the wider population without severe small vessel disease, prior TIA, or stroke. In addition, study in persons with and without small vessel disease may better determine the effect of disconnectivity on dementia, above and beyond the burden of, for example, WMHs.

We aimed to determine the association of global and tract-specific disconnectivity with dementia and cognitive decline in a population-based setting.

Methods

Standard protocol approvals, registrations, and patient consents

The Rotterdam Study has been approved by the medical ethics committee according to the Population Study Act Rotterdam Study, executed by the Ministry of Health, Welfare and Sports of the Netherlands. All participants gave written informed consent.

Study population

This study was embedded within the Rotterdam Study, a population-based cohort study including participants 45 years and older living in Ommoord, a suburb of Rotterdam.¹⁸ The study started in 1990 with 7,983 participants and was extended with 3,011 participants in 2000 and with 3,932 participants in 2006. Participants were examined at baseline with a home interview and an extensive set of examinations in the research center. Follow-up examinations were repeated every 3–4 years. All participants were continuously monitored through electronic linkage of the study database with their own medical records. All details of the study have been described previously.¹⁸ From 2005 onwards, MRI scanning was implemented in the core protocol. Between 2005 and 2011, 5,715 participants without contraindications for MRI (metal implants, pacemaker, claustrophobia) were eligible for scanning, of whom 4,888 (86%) underwent a multisequence MRI acquisition of the brain, and 4,813 (98%) participants completed the diffusion-weighted sequences. We excluded 245 individuals due to technical scanning issues, e.g., failed segmentations, as well as 38 participants with prevalent dementia and 100 participants with insufficient dementia screening at baseline, resulting in a study sample of 4,430 individuals. Of these individuals, 4,317 persons had detailed cognitive assessment at baseline and 3,402 (79%) had repeated assessment during follow-up examination after on average 5.4 (SD 0.6) years.

MRI acquisition and processing

Multisequence MRI was performed on a 1.5T MRI scanner (GE [Chalfont St. Giles, UK] Signa Excite). The imaging protocol has been described extensively elsewhere.¹⁹ The conventional scan protocol consisted of a T1-weighted image, a T2-weighted fluid-attenuated inversion recovery (FLAIR) sequence, and a proton density-weighted image.

Scans were spatially coregistered using rigid registration. Scans were segmented with an automated tissue segmentation approach into gray matter, white matter, CSF, and background tissue,^{20,21} followed by WMH segmentation based on the tissue

segmentation and the FLAIR image.²² Supratentorial intracranial volume (ICV), to correct for head size, was estimated by summing total gray and white matter and CSF volumes.²¹ We visually assessed the presence of infarcts on conventional MRI sequences, and in case of involvement of cortical gray matter, we classified these as cortical infarcts.

Diffusion MRI processing and tractography

For diffusion MRI, we performed a single-shot, diffusion-weighted spin echo echoplanar imaging sequence. Maximum b-value was 1,000 s/mm² in 25 noncollinear directions; 3 volumes were acquired without diffusion weighting (b-value = 0 s/mm²). All diffusion data were preprocessed using a standardized pipeline.²³ In short, eddy current and head motion correction were performed on the diffusion data. The resampled data were used to fit diffusion tensors to compute mean fractional anisotropy (FA) and mean diffusivity (MD) in the normal-appearing white matter, through combination with the tissue segmentation. The diffusion data were also used to segment white matter tracts using a diffusion tractography approach described previously.²⁴ The tract-specific analysis was performed incorporating all voxels of the tract anatomy, both normal-appearing white matter voxels and voxels containing WMHs. Tractography was performed in native space, using standard space seed, target, stop, and exclusion masks as described previously.²⁴ Tractography was performed with PROBTRACKX, a Bayesian framework for white matter tractography, available in FSL (version 4.1.4). Protocols for identifying 15 white matter tracts were defined as described previously and were made available as the autoPTX plugin for FSL (version 0.1.1). The reproducibility of the tractography was 87%, as previously shown.²⁴ The amount of seed points was variable across tracts to achieve a robust sampling of all tracts investigated. The ball and stick diffusion model (BedpostX) estimation and tractography algorithm were run with default settings. We segmented 15 different white matter tracts (12 bilateral, 3 singular) and obtained mean FA and MD in these tracts, with subsequent combination of left and right measures.²⁴ In general, lower FA and higher MD values are considered indicative of lower microstructural integrity and as such reflecting disconnectivity. Missing data for tract-specific measurements due to tractography or segmentation failures were limited to 33–78 participants (0.8%–1.8%) per tract. Tracts were categorized, based on anatomy or presumed function, into brainstem tracts (middle cerebellar peduncle, medial lemniscus), projection tracts (corticospinal tract, anterior thalamic radiation, superior thalamic radiation, posterior thalamic radiation), association tracts (superior longitudinal fasciculus, inferior, longitudinal fasciculus, inferior fronto-occipital fasciculus, uncinated fasciculus), limbic system tracts (cingulate gyrus part of cingulum, parahippocampal part of cingulum and fornix), and callosal tracts (forceps major, forceps minor).²⁴

We obtained tract volumes and tract WMH volumes by combining the tissue and tract segmentations. Tract-specific

WMH volumes were natural-log transformed, to account for their skewed distribution.

Between February 2007 and May 2008, an erroneous swap of the phase and frequency encoding directions for the diffusion acquisition led to a mild ghosting artifact, which was addressed by adjustment in the analysis.²⁴ There was only partial coverage of one of the brainstem tracts (medial lemniscus) due to incomplete coverage of the cerebellum in the field of view, and we used alternative seed masks for tractography and adjustment in the model to overcome this problem.²⁴

Dementia screening and surveillance

All participants were screened for dementia at baseline and during subsequent center visits using the Mini-Mental State Examination (MMSE) and the Geriatric Mental Schedule (GMS) organic level.²⁵ Participants with an MMSE score <26 or a GMS score >0 underwent further cognitive examination and informant interview, including the Cambridge Examination for Mental Disorders of the Elderly. In addition, the entire cohort was under continuous surveillance for dementia through electronic linkage of the study database with medical records from general practitioners and the regional institute for outpatient mental health care. Clinical neuroimaging was used when required for dementia subtype diagnosis. A consensus panel led by a consultant neurologist established the final diagnosis in accordance with standard criteria for dementia (DSM-III-R) and AD (National Institute of Neurological and Communicative Disorders and Stroke–Alzheimer’s Disease and Related Disorders Association). Follow-up until January 1, 2016, was virtually complete (96% of potential person years). Participants were censored at date of dementia diagnosis, death, loss to follow-up, or January 1, 2016, whichever came first.

Assessment of cognitive function

During center visits, all participants underwent routine cognitive assessment comprising a word fluency test (number of animal species within 1 minute), 15-word learning test (immediate and delayed recall of 15 items), letter–digit substitution task (number of correct digits in 1 minute), Stroop test (error-adjusted time in seconds taken for completing the reading, color naming, and interference tasks), and the Purdue Pegboard task for manual dexterity.²¹ To obtain a composite measure of test performance, we calculated the G-factor by principal component analysis,²¹ which explained 49%–54% of variance in cognitive test scores at each examination round in our population. For each participant, Z scores were calculated for each test separately, by dividing the difference between individual test score and population mean by the population SD. Scores for the Stroop tasks were inverted such that higher scores indicated better performance.

Other measurements

Information on smoking habits, educational attainment, and use of antihypertensive and lipid-lowering medication was

ascertained at baseline by structured questionnaires. Blood pressure was measured twice in sitting position using a random-zero sphygmomanometer and the mean of 2 readings was used in the analyses. Total serum cholesterol and high-density lipoprotein (HDL) cholesterol were determined in fasting blood samples. Presence of type 2 diabetes at baseline was determined on the basis of fasting serum glucose level (≥ 7.0 mmol/L) or, if unavailable, non-fasting serum glucose level (≥ 11.1 mmol/L) or the use of antidiabetic medication.²⁶ Body mass index (BMI) was calculated, dividing weight in kilograms by the squared height in meters. History of stroke was assessed by interview, and verified in medical records, and participants were continuously monitored for incident stroke through computerized linkage of medical records from general practitioners and nursing home physicians with the study database. We used the validated Dutch version of the Center for Epidemiologic Studies Depression Scale (CES-D) for assessment of depressive symptoms.²⁷

APOE genotype was determined using PCR on coded DNA samples (original cohort) and using a bi-allelic TaqMan assay (rs7412 and rs429358; expansion cohort). In 179 participants with missing *APOE* status from this blood sampling, genotype was determined by genetic imputation (Illumina 610K and 660K chip; imputation with Haplotype Reference Consortium reference panel [v1.0] with Minimac 3).

Statistical analysis

Analyses included all eligible participants, with the exception of 15 participants whose diffusion measures deviated >7 SDs from the mean, leaving 4,415 participants for analysis. We used Cox proportional hazard models to determine the etiologic association of global and tract-specific diffusion MRI measures (FA and MD) with incident dementia. The proportional hazard assumption was met. We assessed risk of dementia per SD increase in FA and MD. We repeated the analyses (1) for AD only, (2) after excluding participants with prevalent stroke while censoring at time of incident stroke, (3) excluding persons with MRI-defined, subclinical cortical infarcts at baseline, and (4) stepwise excluding the first 5 years of follow-up from the analysis.

We then determined the association of global and tract-specific diffusion MRI measures with change in cognitive performance using linear regression models. Cognitive test scores at follow-up were adjusted for baseline cognitive test results. These analyses were repeated after exclusion of all participants who developed dementia during follow-up.

All models were adjusted for age, sex, education, ICV, white matter volume, and the log-transformed volume of WMHs and the correction for swapping gradients and varying field of view (model I), and in addition for education, depressive symptoms (CES-D score), and cardiovascular risk factors (systolic blood pressure, diastolic blood pressure,

antihypertensive medication, serum cholesterol, HDL cholesterol, lipid-lowering medication, diabetes, smoking, and BMI) and *APOE* $\epsilon 4$ allele carriership (model II). We adjusted for both ICV and white matter volume to take both developmental and neurodegenerative markers into account.

For the tract-specific analyses, we corrected the *p* value (α level of 0.05) for multiple comparisons with the number of independent tests on the basis of the variance of the eigenvalues of the correlation matrix of all 30 variables used in the main analysis (i.e., FA and MD for the 15 tracts). The following formula was used: $M_{\text{eff}} = 1 + (M - 1) (1 - \text{var}(\lambda_{\text{obs}})/M)$, in which *M* is the number of variables, λ_{obs} is the variance of the eigenvalues of the correlation matrix, and M_{eff} is the number of independent variables.^{28,29} This resulted in an M_{eff} of 17.45, which then, using the Šidák formula ($\alpha_{\text{sidak}} = 1 - ((1 - \alpha)^{1/M_{\text{eff}}})$), translated into a significance level of $p < 0.0029$ for the tract-specific analyses with dementia as outcome.²⁸

For the analyses assessing global diffusion MRI measures with the separate cognitive tests as outcome, the above-mentioned method generated a significance level of $p < 0.008$.

All analyses were carried out using SPSS Statistics 21.0 (IBM, Armonk, NY) or R version 3.0.3 (packages GenABEL, survival, stargazer, and data.table).

Data availability

Requests for anonymized data will be considered by the corresponding author.

Results

Table 1 presents the baseline characteristics of the study population. Mean age of the 4,415 participants was 63.9 years (SD ± 11.1 years), and 55.0% were women. During a median follow-up of 6.8 years (interquartile range 5.8–8.0 years), 101 persons developed dementia, of whom 83 had AD.

Lower microstructural integrity, reflected in lower values of global FA and higher values of global MD, was associated with a higher risk of dementia (fully adjusted hazard ratio [HR] [95% confidence interval] per SD increase in FA 0.65 [0.52–0.80] and for MD 1.79 [1.44–2.23]; table 2). Results were similar for clinical AD only, and unaltered after excluding participants with prevalent stroke while censoring at time of incident stroke, or excluding participants with subclinical MRI-defined cortical infarcts (table 2). Stepwise exclusion of the first 5 years of follow-up from the analysis did not alter the risk estimates (figure 1). Further adjustment for hippocampal volume mildly attenuated the effect estimates (MD [HR] for all-cause dementia 1.67 [1.33–2.10], and for clinical AD 1.58 [1.23–2.04]) (data available from Dryad, table e-1, 10.5061/dryad.7wm37vppq).

Table 1 Population characteristics

Characteristics	Values (total n = 4,415)
Age, y	63.9 ± 11.0
Female	2,426 (55.0)
White	3,864 (97.3)
Smoking	
Never	1,367 (31.0)
Former	2,120 (48.0)
Current	928 (21.0)
Lower education	1,266 (28.7)
Middle education	2,107 (47.7)
Higher education	1,042 (23.6)
Systolic blood pressure, mm Hg	140.0 ± 21.5
Diastolic blood pressure, mm Hg	83.2 ± 10.9
Antihypertensive medication	1,573 (35.6)
Total cholesterol, mmol/L	5.5 ± 1.1
HDL cholesterol, mmol/L	1.5 ± 0.4
Lipid-lowering medication	1,113 (25.2)
Diabetes mellitus	531 (12.0)
BMI, kg/m ²	27.4 ± 4.1
CES-D	8 (2–12)
APOE ε4 carriership	1,216 (28.3)
FA	0.34 ± 0.02
MD	0.74 ± 0.03
Intracranial volume, mL	1,142.0 ± 116.4
White matter volume, mL	409.3 ± 60.7
WMHs volume, mL	2.90 (1.6–6.3)

Abbreviations: BMI = body mass index; CES-D = Center for Epidemiologic Studies Depression Scale; FA = fractional anisotropy; HDL = high-density lipoprotein; MD = mean diffusivity × 10⁻³ mm²/s; WMH = white matter hyperintensity.

Continuous variables are presented as mean ±SD and categorical variables as n (%), except for WMHs volume and CES-D score, which are presented as median (interquartile range).

In tract-specific analyses, the strongest associations with dementia risk were observed for MD in the projection tracts, association tracts, and limbic system tracts (per SD increase HR of 2.35 [1.53–3.62] for the superior thalamic radiation, 1.79 [1.36–2.37] for the inferior fronto-occipital fasciculus, and 1.62 [1.41–1.86] for the parahippocampal part of the cingulum, respectively; table 3 and figure 2). Similarly, lower FA in the association tracts and in the limbic system tracts were most profoundly associated with a higher risk of dementia (per SD increase HR 0.59 [0.45–0.76] for the

uncinated fasciculus and HR 0.67 [0.53–0.84] for the parahippocampal part of the cingulum, respectively, in the fully adjusted model; table 3). Similar patterns were seen for a clinical diagnosis of AD only (data available from Dryad, table e-2, 10.5061/dryad.7wm37pvpq).

The association between global white matter microstructure and cognitive decline is presented in table 4. Higher values of global MD were associated with greater decline in global cognition, driven by worse performance on the Word Fluency Test and Stroop reading and interference subtasks. Results were unaltered by exclusion of all incident dementia cases (table 5). Similar associations, albeit somewhat attenuated, were observed for FA.

Discussion

In this longitudinal population-based study, we found that structural disconnectivity is associated with increased risk of dementia and with more pronounced cognitive decline. These associations were most profound for the projection, association, and limbic system tracts, and extended into the pre-clinical phase of the disease.

Longitudinal studies provide higher evidence for causal relations. Our main results provide evidence for the disconnection hypothesis, which states that loss of brain connections precedes cognitive decline and dementia. In line with this hypothesis, our results suggest that disconnectivity plays a role already in the preclinical stages of dementia. The findings in this study also extend results from clinical studies in patients with cerebral small vessel disease to the general population,^{14–17} suggesting that measures of FA/MD may improve prognostic accuracy of existing prediction models to identify persons at high risk of dementia in the community. Furthermore, knowledge of tract-specific effects on cognition and risk of dementia may allow clinicians to better understand why specific patients with only small, but strategically located brain infarcts develop cognitive impairment, and which patients after stroke are most likely to develop dementia.^{30,31}

Various potential pathways could lead to disconnectivity. A vascular pathway has been proposed in which reduction in white matter perfusion, e.g., due to impaired autoregulation, may result in white matter damage.³² Oligodendrocytes might shrink because of hypoxia and ischemia in white matter, with subsequent loss of myelin.^{33,34} However, in our fully adjusted model, we corrected for several cardiovascular risk factors and the estimates did not change substantially. This may be explained by residual confounding (due to age-specific effects of vascular factors or subclinical vascular factors), or a more complex, multifaceted pathway, in which there is a complex interplay of traditional vascular risk factors, hypoxia, and neuroinflammation.³⁵ Inflammation-induced

Table 2 Global white matter microstructure and incident dementia

	Model	FA	MD
All dementia (n = 101)	Model I	0.65 (0.53–0.80) ^a	1.77 (1.43–2.17) ^a
	Model II	0.65 (0.52–0.80) ^a	1.79 (1.44–2.23) ^a
AD (n = 83)	Model I	0.70 (0.55–0.88) ^a	1.71 (1.35–2.16) ^a
	Model II	0.69 (0.54–0.88) ^a	1.76 (1.38–2.24) ^a
Censoring for stroke (n = 98)	Model I	0.65 (0.53–0.80) ^a	1.75 (1.41–2.16) ^a
	Model II	0.64 (0.52–0.80) ^a	1.76 (1.42–2.20) ^a
Exclusion cortical infarcts (n = 97)	Model I	0.63 (0.51–0.78) ^a	1.75 (1.41–2.17) ^a
	Model II	0.61 (0.49–0.77) ^a	1.79 (1.43–2.24) ^a

Abbreviations: AD = Alzheimer disease; FA = fractional anisotropy; MD = mean diffusivity.

Data are presented as hazard ratio (95% confidence interval) per SD increase of FA and MD. Model I: adjusted for age, sex, education, intracranial volume, white matter volume, and the log-transformed white matter hyperintensity volume. Model II: model I and in addition adjusted for Center for Epidemiologic Studies Depression Scale score, cardiovascular risk factors (systolic blood pressure, diastolic blood pressure, antihypertensive medication, serum cholesterol, high-density lipoprotein cholesterol, lipid-lowering medication, diabetes, smoking, body mass index), and *APOE* ε4 allele carriership.

^aSignificant at $p < 0.05$.

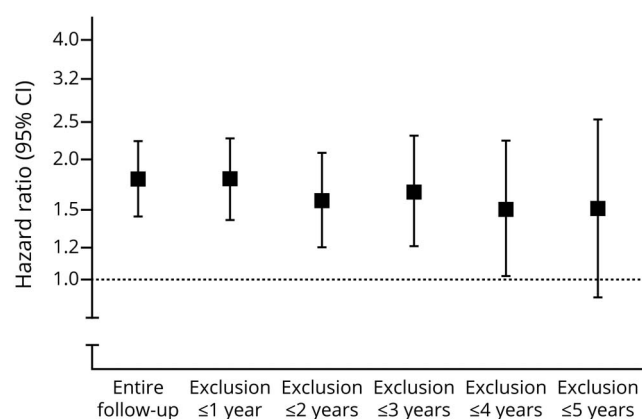
disconnectivity may be caused by inflammation-related cytokines (tumor necrosis factor- α , interleukin-8, interleukin-10, interferon- γ) and growth factors (IGFBP2, PDGF-BB), which have been associated with a lower integrity of myelin sheaths.^{36,37} Yet reverse causality as an explanation for our findings is unlikely since the risk estimates did not change after excluding the first 5 years of follow-up. Also, disconnectivity associated with cognitive decline also in individuals who did not develop dementia during the study duration, suggesting an association already in the preclinical phase of dementia and with normal aging.

We found that structural disconnectivity, indicated by a low FA and high MD throughout the brain, but in particular in

the projection, association, and limbic system tracts, related to a higher risk of dementia. This is in line with previous research in cross-sectional studies that found lower FA in white matter tracts including the association tracts^{38,39} and projection tracts^{40,41} associated with dementia. Lower FA values in limbic system tracts (in particular in the parahippocampal cingulum) and the association with dementia, more specifically AD, has been most consistently reported in previous studies.^{40,42,43}

A small number of studies reported higher FA values in specific regions in AD.^{44,45} This counterintuitive finding may be explained by selective degeneration of a fiber population in regions with crossing white matter tracts, leading to paradoxical higher FA.⁴⁶ MD is therefore thought to be a more sensitive and reliable measure in these crossing fiber regions (and therefore also globally),⁴⁷ and presumably more sensitive to white matter damage.^{11,12} Moreover, in a small group of patients with AD, increases in MD preceded changes in FA, which only occurred in a more progressive disease state.¹¹ Accordingly, in our study we found stronger associations with MD than with FA.

The exact pathologic substrate underlying the changes in FA and MD leading to disconnectivity is unknown. There is pathologic evidence that changes in diffusion MRI measures correlate with myelin damage and axonal count,⁴⁸ that myelin is increasingly suggested as an important factor in AD pathology, and that myelin breakdown is at the core of the earliest changes involved in dementia.⁴⁹ However, the presence of other possible processes such as an increased water content in white matter due to loss of connectivity or inflammation generates difficulties in assigning change in diffusion MRI measures to a specific

Figure 1 Global mean diffusivity and incident dementia, with exclusion of the first 5 years of follow-up

CI = confidence interval.

Table 3 Tract-specific white matter microstructure and incident dementia

White matter tracts	Fractional anisotropy		Mean diffusivity	
	Model I	Model II	Model I	Model II
Brainstem tracts				
Middle cerebellar peduncle	1.05 (0.85–1.30)	1.08 (0.87–1.35)	1.05 (0.85–1.30)	1.04 (0.83–1.30)
Medial lemniscus	1.09 (0.86–1.39)	1.11 (0.86–1.44)	1.06 (0.88–1.28)	1.06 (0.87–1.29)
Projection tracts				
Corticospinal tract	1.17 (0.95–1.44)	1.19 (0.96–1.47)	1.52 (1.13–2.06) ^a	1.52 (1.11–2.08) ^a
Anterior thalamic radiation	0.85 (0.66–1.09)	0.87 (0.67–1.13)	1.68 (1.23–2.30) ^{a,b}	1.73 (1.26–2.38) ^{a,b}
Superior thalamic radiation	1.17 (0.95–1.45)	1.20 (0.97–1.50)	2.29 (1.49–3.52) ^{a,b}	2.35 (1.53–3.62) ^{a,b}
Posterior thalamic radiation	0.69 (0.52–0.90) ^a	0.74 (0.56–0.97) ^a	1.41 (1.15–1.72) ^{a,b}	1.42 (1.15–1.75) ^{a,b}
Association tracts				
Superior longitudinal fasciculus	0.77 (0.60–1.00)	0.79 (0.60–1.04)	1.65 (1.30–2.11) ^{a,b}	1.65 (1.28–2.14) ^{a,b}
Inferior longitudinal fasciculus	0.79 (0.62–1.01)	0.84 (0.65–1.09)	1.73 (1.36–2.21) ^{a,b}	1.69 (1.31–2.18) ^{a,b}
Inferior fronto-occipital fasciculus	0.66 (0.50–0.86) ^{a,b}	0.71 (0.53–0.93) ^a	1.75 (1.34–2.27) ^{a,b}	1.79 (1.36–2.37) ^{a,b}
Uncinate fasciculus	0.60 (0.47–0.77) ^{a,b}	0.59 (0.45–0.76) ^{a,b}	1.67 (1.39–2.00) ^{a,b}	1.73 (1.42–2.10) ^{a,b}
Limbic system tracts				
Cingulate gyrus part of cingulum	0.69 (0.54–0.87)	0.71 (0.55–0.90) ^a	1.55 (1.26–1.92) ^{a,b}	1.58 (1.26–1.97) ^{a,b}
Parahippocampal part of cingulum	0.67 (0.54–0.84) ^{a,b}	0.67 (0.53–0.84) ^{a,b}	1.61 (1.41–1.85) ^{a,b}	1.62 (1.41–1.86) ^{a,b}
Fornix	0.76 (0.59–0.99) ^a	0.78 (0.60–1.02)	1.13 (0.80–1.58)	1.06 (0.75–1.50)
Callosal tracts				
Forceps major	0.77 (0.59–1.00) ^a	0.79 (0.61–1.04)	1.15 (0.93–1.41)	1.12 (0.90–1.38)
Forceps minor	0.78 (0.60–1.01)	0.80 (0.61–1.06)	1.38 (1.12–1.71) ^a	1.39 (1.11–1.75) ^a

Data are presented as hazard ratio (95% confidence interval) per SD increase of fractional anisotropy and mean diffusivity. Model I: adjusted for age, sex, education, intracranial volume, white matter volume, and the log-transformed white matter lesion volume of the investigated tract. Model II: model I and in addition adjusted for Center for Epidemiologic Studies Depression Scale score, cardiovascular risk factors (systolic blood pressure, diastolic blood pressure, antihypertensive medication, serum cholesterol, high-density lipoprotein cholesterol, lipid-lowering medication, diabetes, smoking, body mass index), and APOE ε4 allele carriership.

^a Significant at $p < 0.05$.

^b Significant at $p < 0.0029$.

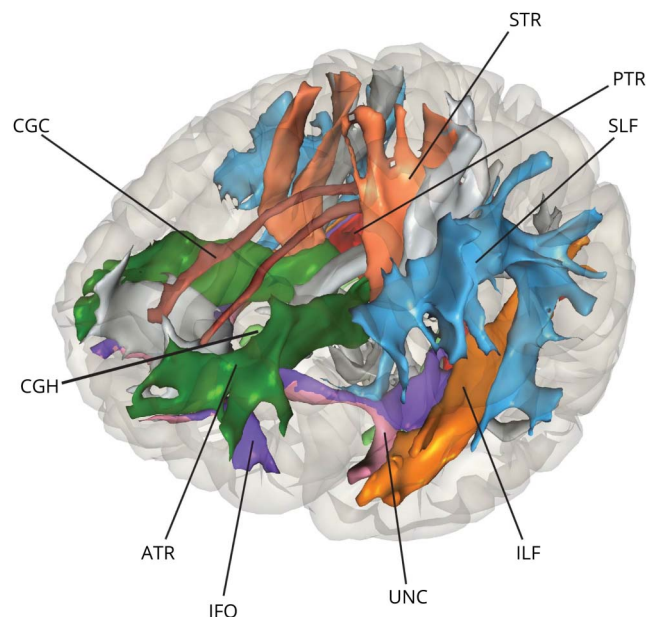
underlying pathologic process causing the observed structural disconnectivity.^{50,51}

Strengths of the study are the population-based setting, the large sample size, the automated publicly available diffusion MRI processing methods that facilitate replication,⁸ and the longitudinal assessment of cognitive performance with meticulous follow-up for dementia. Some limitations need to be considered. First, the averaging of FA and MD measures over the normal-appearing white matter for analyses discards some spatial information. Second, given the long preclinical phase of dementia, our median follow-up time of 6.8 years is still relatively short, and longer duration studies with repeated imaging are required to further map changes in diffusion MRI in the process of neurodegeneration. Nevertheless, our results were unaffected by

excluding the first 5 years of follow-up and independent of macrostructural white matter pathology (i.e., WMH volume). Third, although we found associations similar for all-cause dementia and clinical AD, confirmation of subtype diagnosis by (CSF) biomarkers or pathologic examination was not available and clinical diagnosis of AD has a low specificity for AD pathology. Fourth, we cannot rule out some partial volume effects by CSF contamination driving the observed change in diffusion metrics. Fifth, depression and vascular factors were assessed at baseline only, and some residual confounding by changes over time cannot be excluded.

Structural disconnectivity increases the risk of dementia and more pronounced cognitive decline. Our study suggests that diffusion MRI may be useful in risk prediction.

Figure 2 Tract-specific microstructural integrity and incident dementia



Tracts that were significantly associated with dementia risk are color-coded. Other tracts are presented in gray. ATR = anterior thalamic radiation; CGC = cingulate gyrus part of cingulum; CGH = parahippocampal part of cingulum; IFO = inferior-fronto-occipital fasciculus; ILF = inferior longitudinal fasciculus; PTR = posterior thalamic radiation; SLF = superior longitudinal fasciculus; STR = superior thalamic radiation; UNC = uncinate fasciculus.

Acknowledgment

The authors thank the staff at the Rotterdam Study research center and Frank J.A. van Rooij, data manager.

Study funding

Funding was obtained from the Internationale Stichting Alzheimer Onderzoek 12533, European Union Seventh Framework Programma (FP7/2007-2013) under grant agreement 601055, VPH-Dare@IT (FP7-ICT-2011-9-601055) and the STW perspectief programme Population Imaging Genetics (ImaGene) projects 12722 and 12723, supported by the Dutch Technology Foundation STW, which is part of the Netherlands Organisation for scientific research (NWO) and partly funded by the Dutch Ministry of Economic Affairs. None of the funding sources influenced design or conduct of the study; collection, management, analysis, or interpretation of the data; preparation, review, or approval of the manuscript; or decision to submit the manuscript for publication.

Disclosure

L.G.M. Cremers, F.J. Wolters, M. de Groot, M. Kamran Ikram, and A. Van der Lugt report no disclosures relevant to the manuscript. W.J. Niessen is cofounder, shareholder, and CSO of Quantib BV. M.W. Vernooij reports grants from the Internationale Stichting Alzheimer Onderzoek 12533, European Union Seventh Framework Programma (FP7/2007-2013) under grant agreement 601055, VPH-Dare@IT (FP7-ICT-2011-9-601055), and the STW perspectief programme Population Imaging Genetics (ImaGene) projects 12722 and 12723, supported by the Dutch Technology Foundation STW, which is part of the Netherlands Organisation for Scientific Research (NWO) and partly funded by the Dutch Ministry of Economic Affairs, during the conduct of the study. M. Arfan Ikram reports no disclosures relevant to the manuscript. Go to Neurology.org/N for full disclosures.

Table 4 Global white matter microstructure and cognitive decline

	FA	MD
G-factor	0.02 (−0.004 to 0.041)	−0.04 (−0.07 to −0.01) ^a
Immediate recall	−0.002 (−0.04 to 0.03)	−0.03 (−0.07 to 0.02)
Delayed recall	0.007 (−0.03 to 0.04)	−0.03 (−0.07 to −0.01)
Stroop reading task	0.04 (0.01 to 0.07) ^{a,b}	−0.06 (−0.09 to −0.02) ^{a,b}
Stroop color naming task	0.02 (−0.001 to 0.05)	−0.02 (−0.05 to 0.02)
Stroop interference task	0.04 (0.01 to 0.07) ^{a,b}	−0.09 (−0.12 to −0.05) ^{a,b}
Letter-digit substitution task	0.004 (−0.02 to 0.03)	−0.004 (−0.04 to 0.03)
Word fluency test	0.03 (0.001 to 0.06)	−0.06 (−0.10 to −0.02) ^{a,b}
Purdue pegboard	0.03 (0.005 to 0.06) ^a	−0.04 (−0.07 to −0.00)

Abbreviations: FA = fractional anisotropy; MD = mean diffusivity.

Data are presented as mean difference in Z score (95% confidence interval) per SD increase of FA and MD.

^a Significant at $p < 0.05$.

^b Significant at $p < 0.008$.

Model adjusted for age, sex, education, intracranial volume, white matter volume, the log-transformed white matter lesion volume, Center for Epidemiologic Studies Depression Scale score, and in addition adjusted for cardiovascular risk factors (systolic blood pressure, diastolic blood pressure, antihypertensive medication, serum cholesterol, high-density lipoprotein cholesterol, lipid-lowering medication, diabetes, smoking, body mass index) and *APOE* ε4 allele carrier status.

Table 5 Global white matter microstructural integrity and cognitive decline (after exclusion of all incident dementia cases)

	FA	MD
G-factor	0.01 (−0.01 to 0.04)	−0.03 (−0.06 to −0.001) ^a
Immediate recall	−0.007 (−0.04 to 0.03)	−0.01 (−0.06 to 0.03)
Delayed recall	0.002 (−0.03 to 0.03)	−0.02 (−0.06 to 0.02)
Stroop reading task	0.04 (0.01 to 0.07) ^{a,b}	−0.06 (−0.09 to −0.02) ^{a,b}
Stroop color naming task	0.03 (0.003 to 0.05) ^a	−0.02 (−0.05 to −0.01)
Stroop interference task	0.04 (0.009 to 0.06) ^a	−0.08 (−0.12 to −0.04) ^{a,b}
Letter-digit substitution task	0.005 (−0.02 to 0.03)	−0.004 (−0.04 to 0.02)
Word fluency test	0.03 (0.002 to 0.06) ^a	−0.06 (−0.10 to −0.02) ^{a,b}
Purdue pegboard	0.03 (0.002 to 0.06) ^a	−0.03 (−0.06 to 0.009)

Abbreviations: FA = fractional anisotropy; MD = mean diffusivity.

Data are presented as mean difference in Z score (95% confidence interval) per SD increase of FA and MD.

^a Significant at $p < 0.05$.

^b Significant at $p < 0.008$.

Model adjusted for age, sex, education, intracranial volume, white matter volume, and the log-transformed white matter hyperintensity volume, and in addition adjusted for Center for Epidemiologic Studies Depression Scale score, cardiovascular risk factors (systolic blood pressure, diastolic blood pressure, antihypertensive medication, serum cholesterol, high-density lipoprotein cholesterol, lipid-lowering medication, diabetes, smoking, body mass index), and *APOE* ε4 allele carriership.

Publication history

Received by *Neurology* July 29, 2019. Accepted in final form March 18, 2020.

Appendix Authors

Name	Location	Contribution
Lotte G.M. Cremers, PhD	Departments of Radiology and Epidemiology, Erasmus MC, Rotterdam, the Netherlands	Collected and analyzed the data, interpreted the results, drafted the manuscript, had full access to all the data in the study and takes responsibility for the integrity of the data and the accuracy of the data analysis
Frank J. Wolters, MD	Departments of Epidemiology, Radiology, and Neurology, Erasmus MC, Rotterdam, the Netherlands	Collected and analyzed the data, interpreted the results, drafted the manuscript
Marius de Groot, PhD	Departments of Radiology, Epidemiology, and Medical Informatics, Erasmus MC, Rotterdam, the Netherlands	Collected the data, interpreted the results, drafted the manuscript
M. Kamran Ikram, PhD	Departments of Neurology and Epidemiology, Erasmus MC, Rotterdam, the Netherlands	Designed and conceptualized the study, acquired funding, supervised the study, revised the manuscript for intellectual content
Aad van der Lugt, PhD	Department of Radiology, Erasmus MC, Rotterdam, the Netherlands	Designed and conceptualized the study, acquired funding, supervised the study, revised the manuscript for intellectual content

Appendix (continued)

Name	Location	Contribution
Wiro J. Niessen, PhD	Departments of Radiology and Medical Informatics, Erasmus MC, Rotterdam; Department of Imaging Physics, Delft University of Technology, the Netherlands	Designed and conceptualized the study, acquired funding, supervised the study, revised the manuscript for intellectual content
Meike W. Vernooij, PhD	Departments of Radiology and Epidemiology, Erasmus MC, Rotterdam, the Netherlands	Designed and conceptualized the study, interpreted the results, acquired funding, supervised the study, revised the manuscript for intellectual content
M. Arfan Ikram, PhD	Department of Epidemiology, Erasmus MC, Rotterdam, the Netherlands	Designed and conceptualized the study, interpreted the results, acquired funding, supervised the study, revised the manuscript for intellectual content

References

1. Ferri CP, Prince M, Brayne C, et al. Global prevalence of dementia: a Delphi consensus study. *Lancet* 2005;366:2112–2117.
2. Jack CR Jr, Knopman DS, Jagust WJ, et al. Hypothetical model of dynamic biomarkers of the Alzheimer's pathological cascade. *Lancet Neurol* 2010;9:119–128.
3. Petersen RC. How early can we diagnose Alzheimer disease (and is it sufficient)? The 2017 Wartenberg lecture. *Neurology* 2018;91:395–402.
4. Licher S, Leening MJG, Yilmaz P, et al. Development and validation of a dementia risk prediction model in the general population: an analysis of three longitudinal studies. *Am J Psychiatry* 2019;176:543–551.
5. Reid AT, Evans AC. Structural networks in Alzheimer's disease. *Eur Neuro-psychopharmacol* 2013;23:63–77.
6. Daianu M, Dennis EL, Jahanshad N, et al. Alzheimer's disease disrupts rich club organization in brain connectivity networks. *Proc IEEE Int Symp Biomed Imaging* 2013;266–269.

7. O'Sullivan M, Jones DK, Summers PE, et al. Evidence for "cortical disconnection" as a mechanism of age-related cognitive decline. *Neurology* 2001;57:632–638.
8. de Groot M, Verhaaren BF, de Boer R, et al. Changes in normal-appearing white matter precede development of white matter lesions. *Stroke* 2013;44:1037–1042.
9. Nazeri A, Chakravarty MM, Rajji TK, et al. Superficial white matter as a novel substrate of age-related cognitive decline. *Neurobiol Aging* 2015;36:2094–2106.
10. Vernooij MW, Ikram MA, Vrooman HA, et al. White matter microstructural integrity and cognitive function in a general elderly population. *Arch Gen Psychiatry* 2009;66:545–553.
11. Acosta-Cabronero J, Alley S, Williams GB, Pengas G, Nestor PJ. Diffusion tensor metrics as biomarkers in Alzheimer's disease. *PLoS One* 2012;7:e49072.
12. Acosta-Cabronero J, Williams GB, Pengas G, Nestor PJ. Absolute diffusivities define the landscape of white matter degeneration in Alzheimer's disease. *Brain* 2010;133:529–539.
13. Fu JL, Liu Y, Li YM, Chang C, Li WB. Use of diffusion tensor imaging for evaluating changes in the microstructural integrity of white matter over 3 years in patients with amnesic-type mild cognitive impairment converting to Alzheimer's disease. *J Neuroimaging* 2014;24:343–348.
14. Tuladhar AM, van Uden IW, Rutten-Jacobs LC, et al. Structural network efficiency predicts conversion to dementia. *Neurology* 2016;86:1112–1119.
15. Zeestraten EA, Lawrence AJ, Lambert C, et al. Change in multimodal MRI markers predicts dementia risk in cerebral small vessel disease. *Neurology* 2017;89:1869–1876.
16. Tuladhar AM, Tay J, van Leijns E, et al. Structural network changes in cerebral small vessel disease. *J Neurol Neurosurg Psychiatry* 2020;91:196–203.
17. Williams OA, Zeestraten EA, Benjamin P, et al. Predicting dementia in cerebral small vessel disease using an automatic diffusion tensor image segmentation technique. *Stroke* 2019;50:2775–2782.
18. Ikram MA, Brusselle GGO, Murad SD, et al. The Rotterdam Study: 2018 update on objectives, design and main results. *Eur J Epidemiol* 2017;32:807–850.
19. Ikram MA, van der Lugt A, Niessen WJ, et al. The Rotterdam Scan Study: design and update up to 2012. *Eur J Epidemiol* 2011;26:811–824.
20. Anbeek P, Vincken KL, van Bochove GS, van Osch MJ, van der Grond J. Probabilistic segmentation of brain tissue in MR imaging. *Neuroimage* 2005;27:795–804.
21. Vrooman HA, Cocosco CA, van der Lijn F, et al. Multi-spectral brain tissue segmentation using automatically trained k-nearest-neighbor classification. *Neuroimage* 2007;37:71–81.
22. de Boer R, Vrooman HA, van der Lijn F, et al. White matter lesion extension to automatic brain tissue segmentation on MRI. *Neuroimage* 2009;45:1151–1161.
23. Koppelmans V, de Groot M, de Ruiter MB, et al. Global and focal white matter integrity in breast cancer survivors 20 years after adjuvant chemotherapy. *Hum Brain Mapp* 2014;35:889–899.
24. de Groot M, Ikram MA, Akoudad S, et al. Tract-specific white matter degeneration in aging: the Rotterdam Study. *Alzheimers Dement* 2015;11:321–330.
25. de Bruijn RF, Bos MJ, Portegies ML, et al. The potential for prevention of dementia across two decades: the prospective, population-based Rotterdam Study. *BMC Med* 2015;13:132.
26. Ligthart S, van Herpt TT, Leening MJ, et al. Lifetime risk of developing impaired glucose metabolism and eventual progression from prediabetes to type 2 diabetes: a prospective cohort study. *Lancet Diabetes Endocrinol* 2016;4:44–51.
27. Beekman AT, Deeg DJ, Van Limbeek J, et al. Criterion validity of the Center for Epidemiologic Studies Depression scale (CES-D): results from a community-based sample of older subjects in The Netherlands. *Psychol Med* 1997;27:231–235.
28. Galwey NW. A new measure of the effective number of tests, a practical tool for comparing families of non-independent significance tests. *Genet Epidemiol* 2009;33:559–568.
29. Nyholt DR. A simple correction for multiple testing for single-nucleotide polymorphisms in linkage disequilibrium with each other. *Am J Hum Genet* 2004;74:765–769.
30. Zhao L, Biesbroek JM, Shi L, et al. Strategic infarct location for post-stroke cognitive impairment: a multivariate lesion-symptom mapping study. *J Cereb Blood Flow Metab* 2018;38:1299–1311.
31. Biesbroek JM, Leemans A, den Bakker H, et al. Microstructure of strategic white matter tracts and cognition in memory clinic patients with vascular brain injury. *Dement Geriatr Cogn Disord* 2017;44:268–282.
32. Shi Y, Thrippleton MJ, Makin SD, et al. Cerebral blood flow in small vessel disease: a systematic review and meta-analysis. *J Cereb Blood Flow Metab* 2016;36:1653–1667.
33. Ihara M, Polvikoski TM, Hall R, et al. Quantification of myelin loss in frontal lobe white matter in vascular dementia, Alzheimer's disease, and dementia with Lewy bodies. *Acta Neuropathol* 2010;119:579–589.
34. Aboul-Enein F, Rauschka H, Kornek B, et al. Preferential loss of myelin-associated glycoprotein reflects hypoxia-like white matter damage in stroke and inflammatory brain diseases. *J Neuropathol Exp Neurol* 2003;62:25–33.
35. Heppner FL, Ransohoff RM, Becher B. Immune attack: the role of inflammation in Alzheimer disease. *Nat Rev Neurosci* 2015;16:358–372.
36. Benedetti F, Poletti S, Hoogenboezem TA, et al. Inflammatory cytokines influence measures of white matter integrity in Bipolar Disorder. *J Affect Disord* 2016;202:1–9.
37. Raj D, Yin Z, Breur M, et al. Increased white matter inflammation in aging- and Alzheimer's disease brain. *Front Mol Neurosci* 2017;10:206.
38. Stricker NH, Schweinsburg BC, Delano-Wood L, et al. Decreased white matter integrity in late-myelinating fiber pathways in Alzheimer's disease supports retrogenesis. *Neuroimage* 2009;45:10–16.
39. Damoiseaux JS, Smith SM, Witter MP, et al. White matter tract integrity in aging and Alzheimer's disease. *Hum Brain Mapp* 2009;30:1051–1059.
40. Mayo CD, Mazerolle EL, Ritchie L, et al. Longitudinal changes in microstructural white matter metrics in Alzheimer's disease. *Neuroimage Clin* 2017;13:330–338.
41. Serra L, Cercignani M, Lenzi D, et al. Grey and white matter changes at different stages of Alzheimer's disease. *J Alzheimers Dis* 2010;19:147–159.
42. Zhang Y, Schuff N, Jahng GH, et al. Diffusion tensor imaging of cingulum fibers in mild cognitive impairment and Alzheimer disease. *Neurology* 2007;68:13–19.
43. Kantarci K, Avula R, Senjem ML, et al. Dementia with Lewy bodies and Alzheimer disease: neurodegenerative patterns characterized by DTI. *Neurology* 2010;74:1814–1821.
44. Teipel SJ, Grothe MJ, Filippi M, et al. Fractional anisotropy changes in Alzheimer's disease depend on the underlying fiber tract architecture: a multiparametric DTI study using joint independent component analysis. *J Alzheimers Dis* 2014;41:69–83.
45. Teipel SJ, Stahl R, Dietrich O, et al. Multivariate network analysis of fiber tract integrity in Alzheimer's disease. *Neuroimage* 2007;34:985–995.
46. Douaud G, Jbabdi S, Behrens TE, et al. DTI measures in crossing-fibre areas: increased diffusion anisotropy reveals early white matter alteration in MCI and mild Alzheimer's disease. *Neuroimage* 2011;55:880–890.
47. Jeurissen B, Leemans A, Tournier JD, Jones DK, Sijbers J. Investigating the prevalence of complex fiber configurations in white matter tissue with diffusion magnetic resonance imaging. *Hum Brain Mapp* 2013;34:2747–2766.
48. Beaulieu C. The basis of anisotropic water diffusion in the nervous system—a technical review. *NMR Biomed* 2002;15:435–455.
49. Bartzokis G. Age-related myelin breakdown: a developmental model of cognitive decline and Alzheimer's disease. *Neurobiol Aging* 2004;25:5–18; author reply 49–62.
50. Wood TC, Simmons C, Hurley SA, et al. Whole-brain ex-vivo quantitative MRI of the cuprizone mouse model. *PeerJ* 2016;4:e2632.
51. Duering M, Finsterwalder S, Baykara E, et al. Free water determines diffusion alterations and clinical status in cerebral small vessel disease. *Alzheimers Dement* 2018;14:764–774.